Journal of Water Process Engineering 63 (2024) 105427

Contents lists available at ScienceDirect

Journal of Water Process Engineering

journal homepage: www.elsevier.com/locate/jwpe

Detailed analysis of upgrading a water resource recovery facility to nitrogen removal: Dynamic quantification of power demand, carbon footprint, and operating cost benefits

Mani Firouzian [a,*], Michael K. Stenstrom [b], Diego Rosso [a,c]

[a] Department of Civil and Environmental Engineering, University of California, Irvine, CA, USA
[b] Department of Civil and Environmental Engineering, University of California, Los Angeles, CA, USA
[c] Water-Energy Nexus Center, University of California, Irvine, CA, USA

ARTICLE INFO

Keywords:
Nitrogen removal
Dynamic modelling
Power tariff
Dynamic alpha factor
Greenhouse gas emissions

ABSTRACT

Water resource recovery facilities are major points of electricity demand thus are prime candidates for electricity demand optimization projects. This article summarizes a dynamic analysis of such optimization project consist of upgrading the activated sludge unit of a large water resource recovery facility from carbon oxidizing to nitrogen removing. The changes in the facility electricity demand and efficiency; operating cost; and carbon footprint associated to this optimization project are reviewed in detail here. This detail review demonstrates that although the new configuration increases the facility's aeration requirement, it significantly improves its efficiency. This efficiency improvement, along with significant reduction of waste activated sludge production in the nitrogen removing activated sludge configuration, reduces the facility's overall electricity demand and operating cost. The new configuration is also illustrated to improve the cumulative quality of the facility effluent measured in quality index unit. The overall carbon footprint of the facility is shown to be increased post upgrade, due to higher greenhouse gas emissions associated with microbial activities in the activated sludge unit. Without the direct emissions, the comparison of the facility's carbon footprint presents a reduction in its footprint post upgrade. Hence, upgrades to nitrogen removal can be viewed as energy-savings strategies.

1. Introduction

Water resource recovery facilities (WRRFs) demand significant amount of electricity to operate, and the importance of their energy demand has long been recognized [1]. However, wastewater treatment process remains a minor energy consumer, when compared to other components of the human energy footprint [2]. WRRFs significant power demand makes these facilities desirable candidates for electricity demand reduction projects, especially in light of the recent shifts in the electrical markets. In some areas (e.g., California) this increase in power tariffs can be also explained by growth in photovoltaic electricity generation. This growth has changed the diurnal trend of power demand curves for the electrical grid, turning it into a duck-shaped curve [3,4]. This trend change includes changing the number and duration of diurnal power demand peaks and results in significant hike in the cost of power especially during the peak of demand (16:00–21:00). The higher cost of power during these peak periods are due to limited number of power generation sources that can respond to the short yet sharp ramp up period prior to peak of Duck-Curve and their higher cost of operation [4,5]. The increase in power cost and peak trends has been illustrated in a comparison of few old (legacy) and new power tariffs for Southern California Edison Company (SCE) [6]. These power tariffs graphical comparison has been included in Appendix A of this article and were used in operating cost assessment performed in this study.

The other factor that makes WRRFs an attractive subject for electricity demand optimization projects is their diurnal cycles whose peaks may coincide with that of the power grid's cost depending on the WRRF [6,7]. This coincidence can significantly amplify the effect of recent

* Corresponding author at: Department of Civil and Environmental Engineering, University of California, Irvine, CA, USA.
E-mail address: mfirouzi@uci.edu (M. Firouzian).

https://doi.org/10.1016/j.jwpe.2024.105427
Received 16 December 2023; Received in revised form 24 March 2024; Accepted 1 May 2024
Available online 13 May 2024

electricity tariffs increases in the overall facility operating cost.

Improving the extent of water treatment, not of operating cost savings, has always been the principal focus of WRRFs, [8]. This article reviews the impact of one such optimization project that improves both electricity demand and the extent of treatment at a large WRRF in California. This optimization project consists of upgrading the facility from carbon-oxidation activated sludge to a carbon-oxidation and nitrogen removal (full nitrification and partial denitrification). We used a dynamic model to quantify the differences in aeration efficiency, energy demand, greenhouse gas emissions, and operating cost.

Few decades after transitioning from carbon-oxidation activated sludge to carbon-oxidation and nitrogen removal, this WRRF went through an expansion by adding six additional carbon-oxidizing and nitrogen removing activate sludge process units. This expansion was the focus of another article by the same group of authors as this study. That study could not clearly demonstrate the effect of nitrogen removal on improving the electricity demand, operating cost, and carbon footprint of the facility as its activated sludge processes prior and post expansion removed nitrogen at comparable rates. However, understanding the facility's activated sludge journey prior to that expansion (i.e., transition from carbon-oxidation to carbon-oxidation and partial nitrogen removal) as part of that work, and how that modelling work paved the road for comparison of older configurations of the facility triggered this study. Using the same methodologies and assumptions in both studies would simplify comparing the results of these studies as well as explaining the evolution of this facility activated sludge process to its current form through the past three decades.

For a long time, the additional oxygen required for nitrification has been equated to an expected increase in process operating costs and this attitude has stymied the application of nitrogen removal to many plants. In fact, earlier work by Rosso and Stenstrom (2005) showed that the increase in oxygen transfer efficiency offsets the cost for the additional oxygen (in practical terms, more oxygen is needed but not necessarily more air) [9]. By performing a comparative dynamic analysis of the two process configurations using site-specific aeration performance measurements, in terms of power demand, carbon footprint, and overall operating cost, this study illustrates that increase in aeration efficiency on its own may not overcome the extra electricity demand in the aeration of nitrogen removing scenario, but when combined with the reduction in activated sludge waste production (and consequently its processing and handling electrical demand) the earlier observations are confirmed.

2. Materials and methods

2.1. Facility configuration

The facility discussed in this study is a large coastal WRRF with the average peak influent flow of 5.30×10^5 m^3 d^{-1} (140 MGD) located in California. The facility is equipped with chemically enhanced primary treatment (CEPT) that utilizes ferric chloride and anionic polymers. On average, approximately 20 % of their primary effluent is sent to the facility's two trickling filters equipped with one clarifier each (outside the scope of this research) and the remainder 80 % is treated at the facility's activated sludge units. Most of the facility effluent is used for groundwater recharge and to feed a hydraulic barrier to prevent seawater intrusion. The remainder is discharged into the Pacific Ocean. Since the secondary effluent quality needs to be suitable with the subsequent water reuse operations, effective removal of TSS and BOD is paramount.

In the last two decades, this facility underwent modifications in its activated sludge units' configuration. These included an upgrade from conventional carbon oxidation to nitrogen removal, implemented to improve secondary solids separation and to improve energy-efficiency [10]. To achieve this, the facility's existing carbon oxidation activated sludge (in plug-flow configuration) was modified to a step-feed Ludzack-Ettinger (L-E) configuration without any physical changes of the process units down and upstream of the activated sludge process (Fig. 1).

In the plug-flow configuration, the entire primary effluent went through seven oxidation zones operated in series. Having separate oxidation zones allowed independent; thus, more efficient control of aeration in these zones. To achieve step-feed L-E configuration (i.e., two L-E configurations in series), the aeration in Zones 1A and 3 of the plug-flow configuration was turned off to generate anoxic environment and the effluent to the activated sludge was feed at these two zones as opposed to only one zone (Zone 1A) in the plug-flow configuration by introducing a bypass stream. On average, approximately 40 % of the influent is delivered to the upstream anoxic zone (Zone 1A) and the remainder 60 % is fed mid-way to the downstream anoxic zone (Zone 3).

A small portion of the step-feed activated sludge process

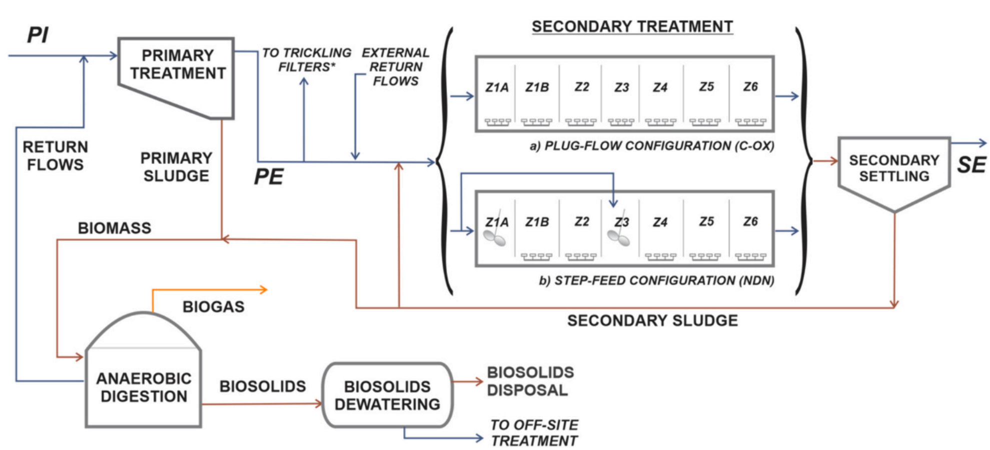

Fig. 1. Facility overall process diagram showing the two activated sludge configurations scenarios: (a) conventional plug-flow activated sludge configuration in carbon oxidation mode and (b) step-feed activated sludge configuration with nitrogen removal (Ludzack-Ettinger or L-E processes). *Following abbreviations were used in this figure: Primary Treatment Influent (PI), Primary Treatment Effluent (PE), Secondary Treatment Effluent (SE), and Zone (Z). **The trickling filter process is outside the scope of this research and zones 1A and 3 of the NDN configuration are anoxic.

configuration's effluent is utilized for the facility's cogeneration system cooling and to backwash the post-secondary microfiltration units. This backwash flow is returned to the secondary influent of this process, as marked in Fig. 1. The presence of nitrate in this recycle stream promotes the operation of this activated sludge process from a strictly L-E to a de facto hybrid L-E/MLE.

All sludge is sent to anaerobic digestion and the resulting biogas feeds the cogeneration plant, which meets most of the energy needs of the overall process and limits the energy importation. Here energy is imported in the forms of natural gas and electricity: the imported natural gas supplements biogas for electricity generation especially during the summer months when electricity costs are higher.

In recent years and in response to the increase in the need for the reuse water, this facility secondary treatment was expanded. For this expansion project, six Modified Ludzack-Ettinger (MLE) activated sludge trains and their associate clarifiers were constructed and added to the facility's existing step-feed L-E activated sludge trains and their secondary clarifiers without changing other process units. The expansion from only step-feed to step-feed and MLE activated sludge was dynamically modelled and reviewed by Firouzian et al. [6]. The model of the facility with only step-feed activated sludge process developed, calibrated, and validated as part of Firouzian et al., 2022 study was used as the starting point to develop the plug-flow scenario model and to model step-feed in this article as explained further in other sections and Appendix B. The Firouzian et al., step-feed model used here was calibrated and validated using plant monthly data for October 2018 through September 2019.

As also explained and demonstrated in Fig. 1, since the process units used for step-feed and plug-flow configuration are the same and only their method of operations was different, the step-feed calibrated and validated model was used as the starting point to develop the plug-flow configuration in this study. The data from historical off-gas testing of the plug-flow configuration by the authors of this publication was used to modify and calibrate the step-feed model to plug-flow.

As also illustrated in Fig. 1 in addition to the bypass feed stream, the difference between these two activated sludge configurations is operation of their 7 aeration zones. This difference was accounted for in the model by using different numbers of air diffusers pursuant to the historical off-gas tests data for plug-flow configuration. The waste activated sludge (WAS) dynamic flow trend of this activated sludge configuration was also adjusted pursuant to the off-gas data to achieve its significant lower solid retention time (SRT) comparing to step-feed. Hourly SRT of plug-flow scenario ranged from 1 to 1.5 days comparing to 3.9 to 6.5 days for step-feed's during the 12 months study period.

2.2. Field data collection, modelling tool, and protocol

The dynamic process model was developed using BioWin 6.1 (EnviroSim; Hamilton, ON) and the Good Modelling Practice protocol [11]. The influent dynamic profile developed for modelling the current facility in Firouzian et al., 2022 [6] illustrated in Fig. B.1 of Appendix B, was used here so the result of this study could be also compared with that model's (see discussion). Process equipment size and configuration data used for developing the process models are summarized in Appendix C.

Field oxygen transfer efficiency data in process conditions (oxygen transfer efficiency or OTE, %) was measured through a series of off-gas tests pursuant to the American Society of Civil Engineers (ASCE) testing protocol [12]. The α factor calculated by ratioing the field OTE values corrected to standard condition (i.e., the αSOTE, %) to that of clean water (SOTE, %) from the air diffusers' manufacturer was used as one of the model inputs. The alpha factors derived from these field-testing campaigns are summarized in Table 1.

Table 1
Ranges of alpha factors derived from field-testing used to describe the aeration dynamics in the activated sludge reactors in this study. The alpha factor is not defined for anoxic zones.

Step-feed activated sludge configuration (NDN)							
Zone:	Zone 1A	Zone 1B	Zone 2	Zone 3	Zone 4	Zone 5	Zone 6
Max	Anoxic	0.66	0.79	Anoxic	0.91	0.94	0.75
Min	Anoxic	0.37	0.66	Anoxic	0.55	0.62	0.65
Average	N/D	0.48	0.74	Anoxic	0.69	0.83	0.71

Plug-flow activated sludge configuration (C-OX)							
Zone:	Zone 1A	Zone 1B	Zone 2	Zone 3	Zone 4	Zone 5	Zone 6
Max	0.30	0.30	0.30	0.26	0.28	0.29	0.27
Min	0.23	0.23	0.28	0.24	0.25	0.25	0.26
Average	0.26	0.26	0.29	0.25	0.26	0.28	0.27

In the activated sludge process aeration basins, surfactants molecules sorb onto surface of the air bubbles generated to oxidize the wastewater constituent and inhibit transfer of the oxygen from the air inside these bubbles to the wastewater. In denitrification process, denitrifying microorganisms selectively consume surfactants as carbon source. Thus, they reduce surfactants' negative effect on oxygen transfer which is quantified by alpha as explained in this section [9,13]. This explains the higher alpha factors (i.e., more effective oxygen transfer) of NDN scenario comparing to C-ox in Table 1.

To develop a dynamic model for the two activated sludge configurations in this study, dynamic alpha trends for each aeration basin of these two configurations were needed. The simulation software used here did not calculate alpha (as in Bencsik et al., 2022 [14]). However, the simulator allowed the user to enter a time-dependent diurnal alpha schedule for each aeration basin. Pursuant to the method used in the modelling effort by Firouzian et al., 2022 [6], these dynamic hourly trends for alpha were derived utilizing Jiang-Garrido-Baserba dynamic alpha equation [15] for each aeration basin, where alpha is a function of the COD applied to the process. The ratios of each hourly-to-average alphas for the entire study period were applied to the field average alpha factors in Table 1 to develop the facility specific dynamic alpha trends.

To compare the carbon footprint of step-feed and plug-flow scenarios, greenhouse gas (GHG) emissions associated to: grid's electricity import; combustion of biogas and imported natural gas; activated sludge biological treatment; sludge digestion; and biogas fugitive emissions were accounted for. The emissions associated with the electricity imported from the grid was estimated using the dynamic grid electricity's hourly average carbon intensity trends prepared by Firouzian, et al., 2022 which were calculated from the data obtained from the California Independent System Operators [16]. U.S. EPA protocol was utilized for calculating the combustion emissions [17]. GHG from biological processes in activated sludge and digesters were quantified by the simulation software [18].

Assuming the plant metering system being used as the first mean to identify biogas leaks and initiating repair at WRRFs, the leaks hidden within the metering accuracy limit could be assumed to continue and not addressed. Therefore, metering accuracy level (% Error) was used as the basis for continuous biogas fugitive emissions. ±1 % is the average of accuracy of the common flowmeters used at wastewater treatment plants under ideal conditions defined by meter manufacturer [19]; thus, fugitive methane emission associated with biogas leak was assumed to be 1 % of the total methane generation in the digesters. It needs to be noted that the corrosive nature of biogas, the error associated with other components of metering system (e.g., data transmitters, thermocouple, etc.), and lack routine calibration of meters, result in the inaccuracy of biogas meters to be significantly greater than the ideal limits provided by manufacturers.

Total operating cost of these scenarios were also calculated by summing up the cost of: electricity and natural gas imports; chemicals used for enhancing primary treatment, sludge thickening and biosolids dewatering; and biosolid disposal. Southern California Edison's (SCE's) Time-of-Use power rates and tariffs presented in SCE Schedules TOU-8-S and TOU-8-RTP-S [20] and similar averaging assumptions of Firouzian, et al., 2022 were used to calculate the cost of power import. Except for the anionic polymers used for CEPT whose cost (32.13 USD per 1000 m^3 of primary treatment influent) was obtained from the chemical provider (NSF Polydyne Inc.;Riceboro, GA), the costs of other chemicals and natural gas fuel used for the treatment as well as sludge disposal cost were calculated using the software defaults [18].

2.3. Normalization of results

To compare fairly the result of modelling for these two scenarios' electric power demand, GHG emissions, and operating cost, these results are normalized to different functional units representing the extent of treatment. These normalization methods include: 1) normalization per unit influent flow; 2) normalization per unit of activated sludge theoretical oxygen requirement; and 3) normalization per unit of quality index removal [21,22]. Each normalization has different implications and interpretation; hence, some elaboration is warranted.

Normalization to the facility influent flow treated was utilized here to compare the net and total power demand as well as effluent quality index or EQI (as defined at the end of this section and Appendix E) of these two scenarios. This is due to the fact that the influent flow values utilized for modelling of these two scenarios were slightly different. The normalized net and total power demand to influent flow are referred to as net and total electrical energy intensities in this article. The theoretical oxygen requirements, defined as the theoretical amount of oxygen required for removal of carbonaceous material and oxidation of ammonium (i.e., aqueous form of ammonia) to nitrate, are the entity used here to normalize and compare the electricity demand in the activated sludge units of these scenarios. This normalized electricity demand is referred to as activated sludge energy-intensity.

The quality index removal (QIR), defined as the removal of the effluent quality index or EQI (as defined in Jeppsson et al., 2007). The QIR is the weighted sum of the difference between TSS, TKN, COD, nitrate, and BOD in the facility influent (influent quality index: IQI) and effluent (effluent quality index: EQI). This weighted sum is a more realistic representation of the environmental impact of these constituents in wastewater [21,22]. The QIR was utilized to normalize and compare the net and total electricity demand; GHG emissions; and operating cost. More details about these quality index parameters and their equations have been included in Appendix E.

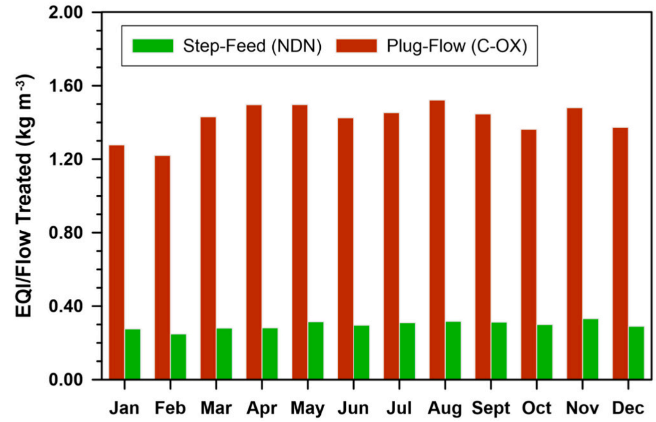

Fig. 2. Monthly effluent quality index (EQI) normalized per unit flow treated, for the plug-flow and step-feed scenarios. Note that lower values in the vertical axis imply better quality of effluent water.

3. Results and discussion

3.1. Effluent quality

To simplify the comparison of the effluent quality for these scenarios, a cumulative comparison was performed utilizing effluent quality index (EQI) [21,22] as opposed to comparing the effluent individual pollutants. A more detailed and graphical comparison of these effluent constituents has been provided in Appendix D. Mind that EQI is a weighted measure of pollution and therefore a higher EQI value corresponds to lower effluent quality. The influent flow values utilized for modelling these two scenarios are slightly different; thus, the calculated EQI for these scenarios' comparisons have been normalized to the facility's influent flow to account for this slight difference and to have a fair comparison of these scenarios. Comparing the normalized monthly EQI for the two scenarios in Fig. 2 illustrates the plug-flow's EQI to be more than quadruple of the step-feed's. In other words, the optimization project here significantly improves the overall quality of the facility effluent and lowers its environmental impact.

The definition of the EQI assigns a low weight to the TSS in the effluent, considering its reduced impact on the receiving water body, when compared to more reactive nitrogenous species such as ammonium and nitrate. This elucidates the significantly higher EQI in the plug-flow scenario that removes significantly smaller amount of nitrogen comparing to step-feed's despite plug-flow's smaller effluent TSS. It needs to be noted, however, that the removal of TSS is of more importance for this facility as its effluent is undergoes microfiltration for water reuse (the energy demand of micro filtration is selectively affected by suspended solids).

3.2. Power demand comparison

Fig. 3 illustrates the overall annual total power demand breakdown for the main treatment processes of each scenario.

Fig. 3 illustrates comparable total average daily power demand normalized by unit of plant influent flow (<0.7 % increase) as well as the power demand breakdown for the main unit processes in these two scenarios. The comparison of the main process units shows that the upgrade of nitrogen removal does not change the power demand of most of this facility's process units. The only process units that are observed to

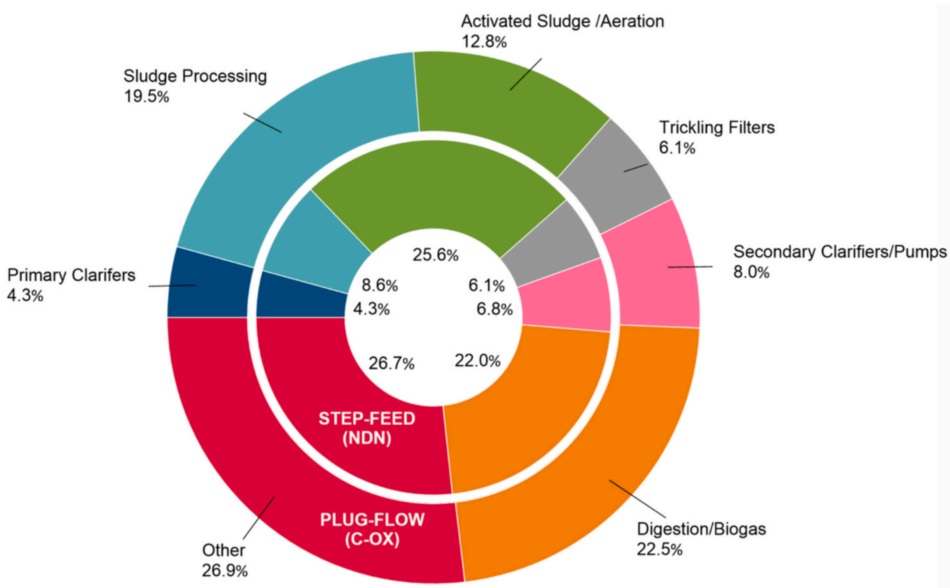

Fig. 3. Total electricity demand breakdown by treatment process for plug-flow and step-feed scenarios. The total average daily electricity demand of NDN (step-feed) and C-ox (plug-flow) scenarios normalized to their influent flows are 4.93×10^{-1} kWh m^{-3} and 4.89×10^{-1} kWh m^{-3}, respectively.

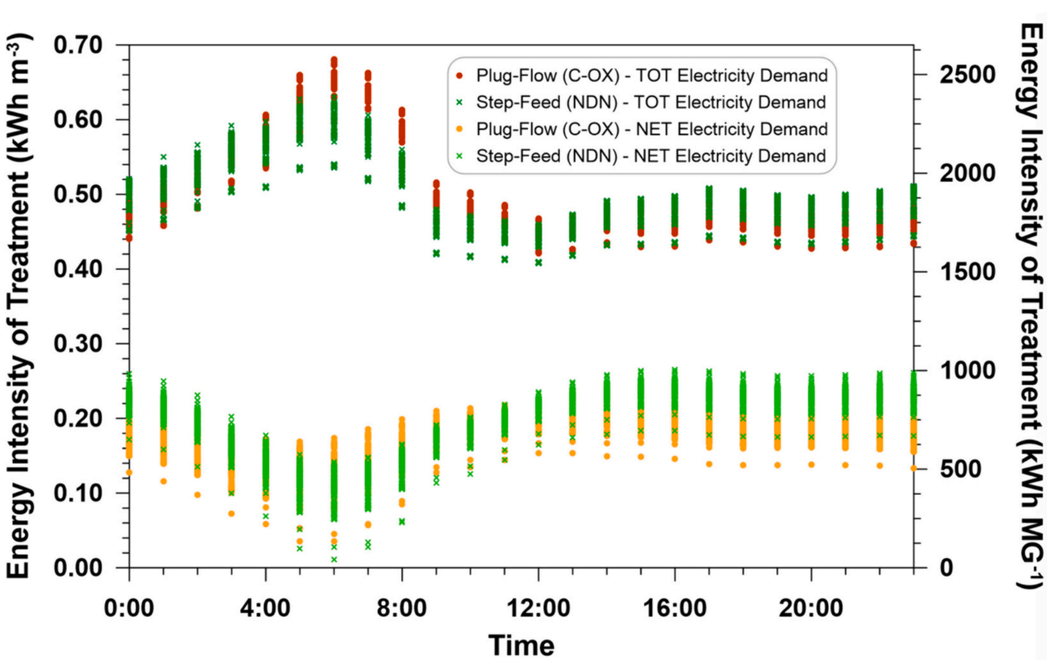

Fig. 4. Dynamic net and total treatment electrical energy intensities (electricity demand normalized to plant influent flow) for plug-flow and step-feed scenarios. Both Y-axis apply to the data points plotted and the data points are for each day of the calendar year calculated at the same hour.

experience a change in their electricity demand are sludge processing (i.e., sludge thickening and biosolids dewatering and loading) and activated sludge aeration.

A closer look at Fig. 3 shows that the sum of sludge processing's and activated sludge's power demand remains unchanged after converting the activate sludge from C-ox to NDN. In other words, addition of nitrogen removal in step-feed (NDN) configuration only diverts some of the electricity demand from sludge processing of the plug-flow (C-ox) configuration to the activated sludge aeration in step-feed. This invalidates the myth suggesting larger power demand in WRRFs that remove nitrogen in comparison with only carbon oxidizing facilities and confirms the earlier observations by Rosso and Stenstrom (2005; 2007) [9,10].

3.3. *Electrical energy-intensity comparison*

Dynamic net and total electrical energy intensity are compared in Fig. 4. This figure illustrates that the improved effluent quality after

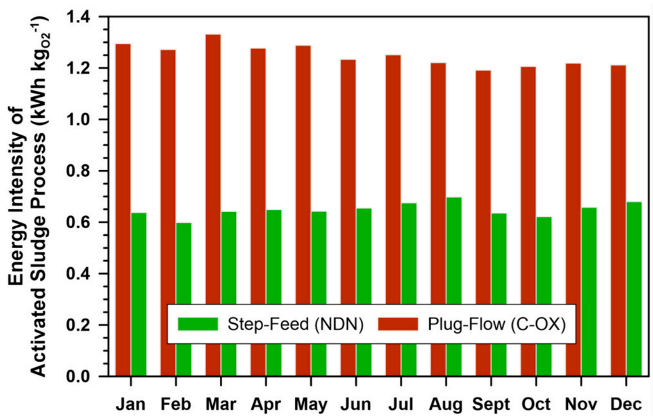

Fig. 5. Comparison of the activated sludge energy intensity (defined as the electrical demand per unit of theoretical oxygen requirements) for plug-flow (C-ox) and step-feed (NDN) scenarios.

upgrade to NDN portrays the realistic image of the energy intensity of the process, with a change in total energy intensity ranging from −0.07 to 0.05 kWh m^{-3}. A closer comparison of total energy intensities here shows that NDN has larger total energy intensity than C-ox for 58 % of the study period while C-ox is larger for the remaining 42 %. This configuration change also results in changes in net energy intensity ranging from −0.04 to 0.07 kWh m^{-3}. During 74 % of the study period NDN's net energy intensity is higher than C-ox. In short, upgrading to NDN can be seen as an energy-efficiency measure, if we take into consideration the increased load removed.

Fig. 4 illustrates that the total electrical energy intensity is minimum (or close to it) at the peak of the facility influent load (between 12:00 and 23:00) while the net is maximum. This is despite the fact that both net and total electricity demands' hourly trends follow the same pattern as of the influent flow's and the net power demand energy intensity's and all peak between 12:00 and 23:00. The reciprocal or reversely arranged trend of total and net electrical energy intensities in this figure can be explained to be due to different magnitude of each of the net and total power demand hourly values (net < total) comparing to same hourly influent flow value they are divided by to calculate the energy intensities (net and total) for that hour. Since the plant influent flow does not fully capture the extent of the removal for its different constituents, other normalization methods were used for the electricity comparison in the following sections.

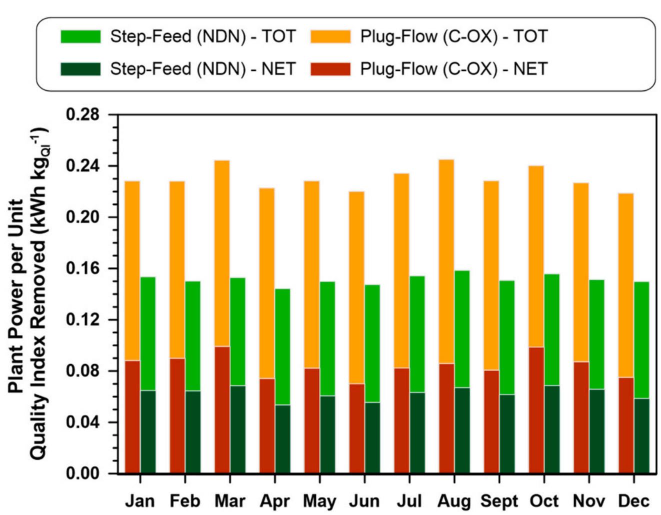

Fig. 6. Facility total and net power demand normalized per unit quality index removal for plug-flow (C-ox) and step-feed (NDN) scenarios.

3.4. Activated sludge energy intensity comparison

Since aeration power demand is a main concern when upgrading to nitrogen removal, the comparison in aeration power demand is conducted using activated sludge energy intensity in Fig. 5.

As Fig. 5 demonstrates, when the amount of load removed (in terms of oxygen demand) is used for normalization, the activated sludge energy-intensity after NDN is less than half than that of C-ox. This higher aeration efficiency can be explained by larger alpha factors after NDN as demonstrated in Table 1. As explained in the previous section, the denitrification process selectively removes surfactants in the anoxic compartment, hence increases the alpha factor with consequent decrease of process energy cost [9].

3.5. Electricity demand normalized per unit quality index removal

To account for the facility's overall extent of removal in the whole facility, net and total power demand of each scenario for each month of the year is normalized per unit quality index removal (QIR) and compared in Fig. 6.

Fig. 6 demonstrates that both total and net electricity demand normalized per unit QIR are lower for the NDN scenario by 31–37 % and 21–31 %, when compared to C-ox, respectively. This slightly lower normalized power savings associated to upgrade to NDN when comparing net to total electricity demand in this figure (31–37 % vs 21–31 %,) is due to roughly 13 % higher biogas productions in the C-ox scenario. This higher production of biogas results in higher in-house electricity generation that compensates a portion of the larger power savings observed in the normalized total power demands in Fig. 6.

The higher biogas production in the C-ox scenario can be explained by this scenario's higher biodegradable or digestible organics contents of secondary sludge as a result of its low mean cell residence time (MCRT) and its higher waste activated sludge (WAS) flow.

3.6. Greenhouse gas emissions

Fig. 7 compares the daily greenhouse (GHG) emissions breakdown by source types for both scenarios. This figure demonstrates activated sludge and digester process emission to be one of the major sources of the GHG emissions which consists of the CO_2, CH_4, and N_2O emissions generated by activated sludge and CO_2 emission generated by the digester. The combustion emission (biogas and natural gas) is another major source of emissions followed by CO_2 emissions associated with power importation and biogas fugitive leak CH_4 emissions.

The ranking order of these two major contributing sources to the facility's total carbon-footprint are reversed for the two scenarios compared in this article. In the NDN configuration, the combined emissions from activated sludge and digestion are the largest contributor while they are the second in magnitude after biogas and natural gas combustion in the C-ox scenario.

Fig. 7 demonstrates that the upgrade to NDN has increased the facility's overall daily GHG emissions by almost 43 %. The higher sludge retention time of NDN results in more respiration and, during both nitrification and denitrification, in the direct emission of N_2O, resulting in more than triple of the C-ox emissions. Migration of the activated sludge to NDN also increases the grid's electricity import GHG emissions by 17 %, a compounding effect of aeration electrical energy demand reduced in-house electricity generation (due to the 6 % lower biogas production). This modification; however, reduces the total combustion (biogas and natural gas) and fugitive emissions by 11 % and 6 %, respectively, by lowering the facility's biogas production. Reduction of the WAS in the NDN (step-feed) scenario also reduces the thermal energy demand for heating up the digesters' influent. This thermal energy demand reduction translates into allocation of its associated fuel savings to in-house power generation in the step-feed scenario and lowering the electricity imports emissions. Accounting for only anthropogenic GHG

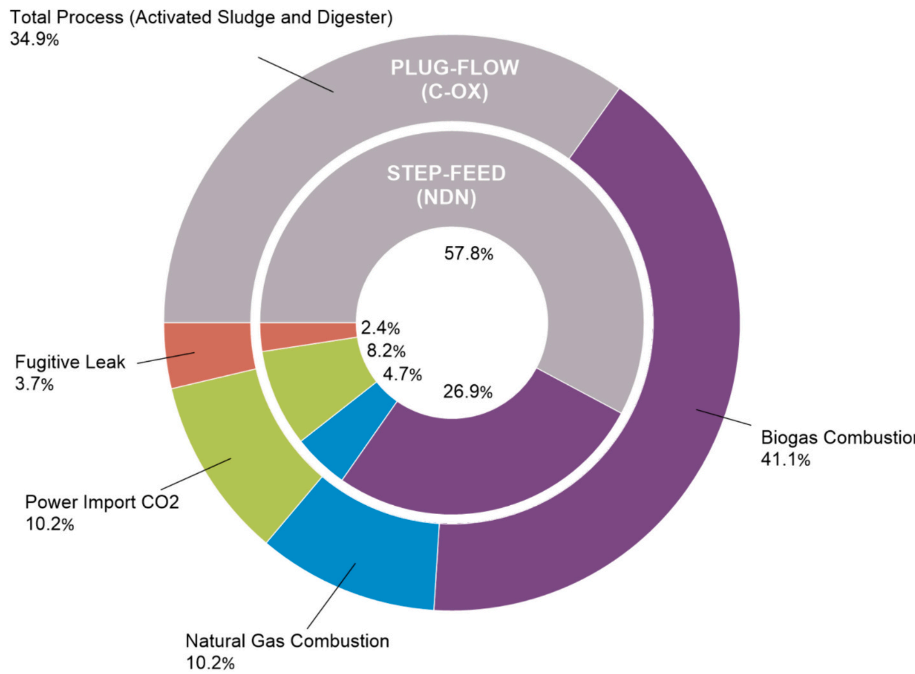

Fig. 7. Greenhouse gas emissions breakdown by source type for C-ox (plug-flow) and NDN (step-feed) scenarios. The total average daily emissions normalized per unit influent flow treated for the step-feed and plug-flow scenarios are 0.62 $kgCO^2eq\ m^{-3}$ and 0.43 $kgCO^2eq\ m^{-3}$, respectively.

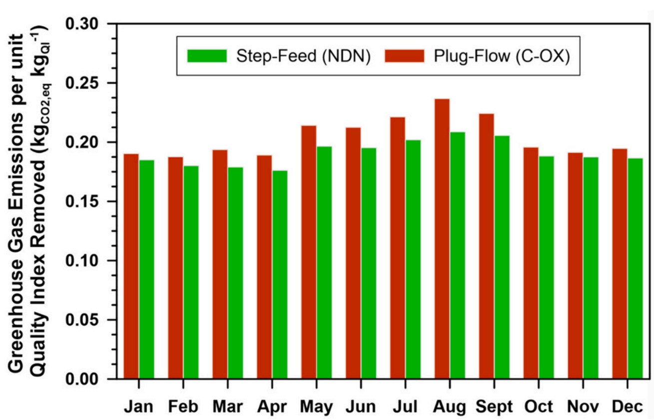

Fig. 8. Greenhouse gas emissions to quality index removal ratio comparison for C-ox and NDN scenarios. Note that after normalizing per unit effluent quality reached (i.e., per unit QIR), the overall GHG emissions are lower for the NDN scenario.

emissions, which can also include part of the CO_2 from respiration due to the presence of fossil carbon in the plant's influent [23], the upgrade to NDN results in an average 17 % increase of the facility's GHG emissions.

Care must be used when comparing the absolute value of emissions across scenarios with different levels of treatment. It is possible to mistake the higher emission with lower value for the process performing more treatment, but in fact the overall environmental health benefits from the improved effluent quality. To compare fairly the emissions, a normalization by overall unit effluent quality achieved (i.e., by unit QIR) is useful, showing that the monthly specific emissions are actually lower for NDN by 2–12 % (see comparison in Fig. 8).

This figure also portrays slight seasonal trend in normalized GHG emissions with larger and lower ratios for both scenarios occurring during hot (May through September) and cold months (October through April) of the year, respectively. The higher normalized emissions in the hotter months can be explained by the increase of in-house power generation using natural gas in summer months in response to higher grid electricity tariffs and lower efficiency of the blowers in the hotter months. This lower efficiency is due to positive correlation between blowers' energy demand required to deliver unit airflow to AS units and ambient air temperature translating into higher electricity demand and its associated GHGs in the hotter months of the year.

3.7. Total operating cost

Similar to GHG emissions, the total operating costs (as explained in Materials and methods section) are normalized per unit QIR to account for the extent of overall treatment. To compare the two scenarios, the ratio of the operating cost for the C-ox to the NDN is calculated. Since each treatment scenario would have 6 power tariff sub-scenarios, the ratios of normalized total operating costs for the two scenarios are grouped by month in Fig. 9 to simplify the comparison here. Details on the different power tariffs are reported in Appendix A.

Fig. 9 illustrates that the normalized total operating cost of the C-ox (plug-flow) is more than double of the NDN's (step-feed's) for all the tariff structures. Therefore, modification to step-feed has provided a great amount of operating cost savings in addition to providing better overall effluent quality for this facility. This figure also demonstrates that the effect of tariff structure on the outcome of this operating cost comparison is only considerable during the grid's summer months (June through September).

The NDN higher electricity imports, due to lower biogas production and slightly higher electricity demand, result in higher imported electricity cost comparing to the C-ox scenario. However, the C-ox's additional operating cost associated with higher WAS production in the activated sludge will significantly overcompensate the step-feed's higher electricity import cost. In fact, the higher WAS flow in C-ox results in higher usage and cost of chemical additives used in sludge thickening and dewatering, higher thermal energy demand in digesters for sludge pre-heating, and larger disposal costs of biosolids. The most significant of all these three is the higher chemical additives cost. Since the primary treatment was assumed and configured to be the same for both scenarios, the chemical usage for enhancing its performance and its sludge thickening and dewatering normalized to total QIR is expected to be the same for both scenarios. Therefore, the significant chemical usage cost

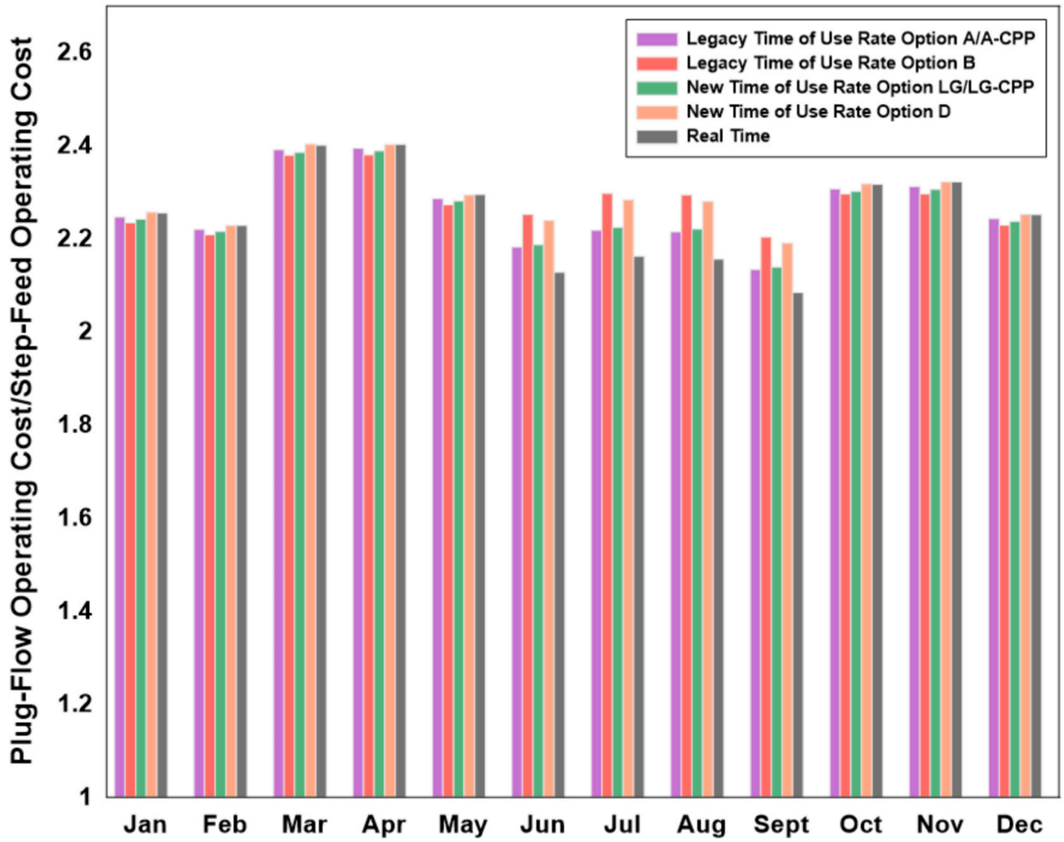

Fig. 9. Total operating cost per unit quality index removal for C-ox (plug-flow) and NDN (step-feed) scenarios, applying SCE five power tariffs (Appendix A). The results are presented as dimensionless ratios, with the NDN configuration in the denominator. Annual total operating cost to unit quality index removal ratio calculated using the average of these 5 tariffs annual electricity cost for C-ox and NDN configurations are 99.36 USD per metric ton and 43.90 USD per metric ton respectively.

difference observed here can be narrowed down to the secondary treatment's waste sludge dewatering and thickening.

The WAS flow in the C-ox scenario is on average more than five times that of NDN. This significant difference results in the same order of magnitude higher chemical additive cost (five-fold) in the secondary sludge thickening process of C-ox scenario where the additive usage and its cost are directly calculated from the WAS flow using a constant dose.

The higher cost of the grid's electricity in the summer months (June–September) amplifies the NDN's higher electricity import cost resulting in further compensation of the C-ox's higher overall operating cost. This elucidates the slight decrease in the cost ratios illustrated in the Fig. 9 in the summer months.

3.8. Extension to other locations

This work focuses on a facility sited in a 2-season climatic zone. It is important to relate these results to other areas with 4-seasons or with different geographical setting. When winter temperatures drop substantially and require longer MCRTs to achieve the same extent of treatment, the difference between C-ox and NDN would be more pronounced. A sensitivity analysis on the effects of MCRT and wastewater temperature on the comparative results should be included in future studies. Recently, the implications on technology selection for secondary treatment of the facility's elevation were addressed by Baquero-Rodriguez et al., 2022 [24]. As elevation increases, the partial pressure of oxygen in atmospheric air decreases and with it the driving force for oxygen transfer, resulting in an increase in energy requirements for aeration. The higher the elevation, therefore, the larger the advantage for the configuration with less oxygen requirements per unit treatment achieved (in this case, NDN).

4. Summary and conclusions

A process model was used to compare the two scenarios of carbon oxidation (C-ox) and the subsequent upgrade to nitrification and denitrification (NDN) at a large treatment facility. For fair and close comparison of the evaluation metrics, the energy-intensity, greenhouse gas emissions, and operating costs are reported in both absolute terms and are also normalized per unit extent of the treatment. There are different ways to define the extent of treatment and here we used treated water volume, removed load, and effluent quality index.

The comparison of these normalized values shows higher aeration energy efficiency in the activated sludge unit after NDN upgrade and presents this scenario as the more energy-efficient option to carbon oxidation. The higher aeration energy efficiency observed in NDN is due to selective removal of surfactants in the anoxic denitrification reactor.

Comparing the overall greenhouse gas emissions of the facility prior and post upgrade to nitrogen removal, normalized per unit effluent quality index removal, we show a decrease in emissions. A comparative analysis of the facility's total operating cost using different electricity tariff structures also presented significant cost saving after upgrade to nitrogen removal, mostly due to reduction of sludge and biosolids processing and handling costs in the NDN scenario, given its lower sludge age (hence, lower secondary sludge production). Conversely, the higher secondary sludge production in the C-ox scenario produced higher biogas production, resulting in higher in-house power generation and consequently in lower power imports and associated costs. However, these savings could only offset part of this scenario's higher cost of sludge and biosolids processing and disposal. Furthermore, we should remark that the benefits of additional biogas production prior to upgrade to NDN are not applicable to facilities without biogas recovery.

CRediT authorship contribution statement

Mani Firouzian: Writing – original draft, Software, Methodology, Formal analysis, Data curation. **Michael K. Stenstrom:** Writing – review & editing, Investigation, Conceptualization. **Diego Rosso:** Writing – review & editing, Validation, Supervision, Methodology, Investigation, Conceptualization.

Declaration of competing interest

The authors declare that they have no known competing financial interests or personal relationships that could have appeared to influence the work reported in this paper.

Data availability

The data that has been used is confidential.

Acknowledgements

The authors thank the utility personnel who supplied data and information.

Funding

This research did not receive any specific grant from funding agencies in the public, commercial, or not-for-profit sectors.

Appendix A. Southern California Edison power tariff applicable to a WRRF

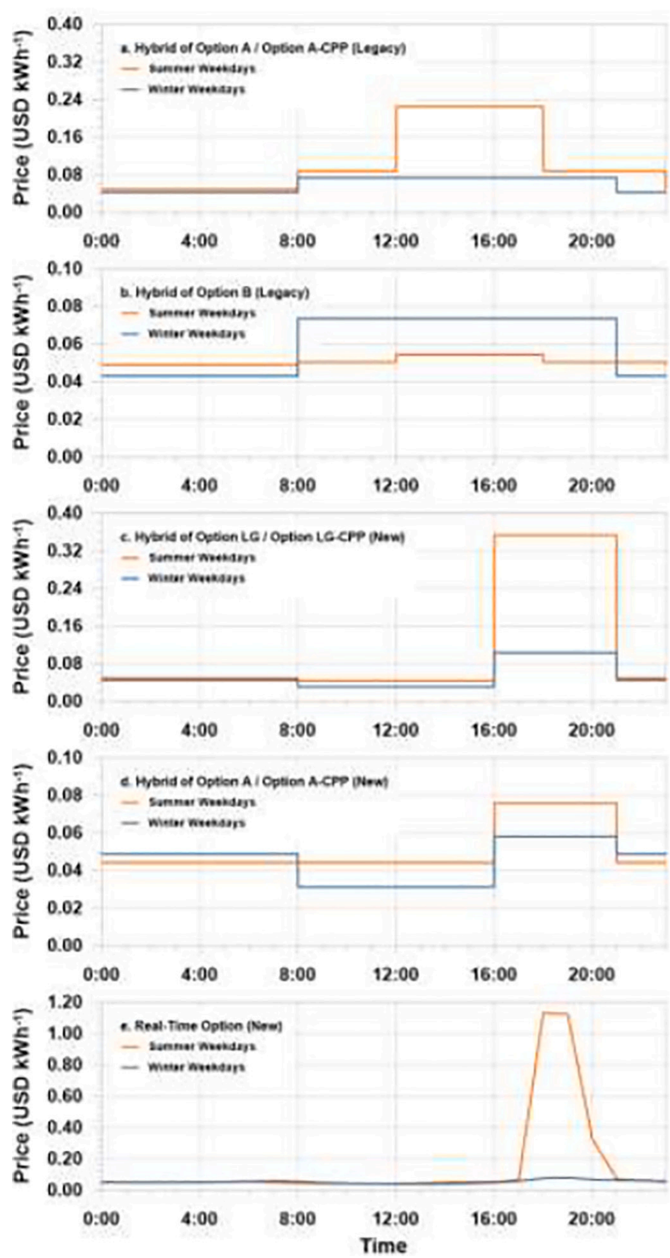

Fig. A.1. (a) to (d). SCE's new and old (legacy) time-of-use schedule for facilities with internal generation capacity and with demand of >500 kW (TOU-8-S) for weekdays derived from average of fee scheduled for 2–50 kV and >50 kV grids [Effective as of March 1, 2019]. (e). SCE's current real-time schedule for facilities with internal generation capacity and with demand of >500 kW (TOU-8-RTP-S) for weekdays derived from average of fee scheduled for 2–50 kV and >50 kV grids [Effective as of March 1, 2019] [6,20].

Appendix B. Current facility configuration modelling method

BioWin 6.1 (EnviroSim; Hamilton, ON) and the Good Modelling Practice protocol [11] was utilized to perform dynamic modelling of the current expanded facility. The steps defined and utilized by Firouzian et al., 2022 were followed to develop the dynamic simulations for the step-feed and plug-flow scenarios in this study as summarized in this appendix [6].

The monthly average process data from the facility was utilized for calibration and validation of this model. Specifically, October through December 2018 monthly data were used for calibration and January through September 2019 data for validation. Dynamic hourly influent profiles were derived from these monthly averages as explained in more details in this section. The influent fractions adjusted to match the concentrations of the field data. Default values in the simulation software [18] were used here unless otherwise described in Appendix C.

In addition to the process units, electricity demand was also calculated for the main equipment units (e.g., pumps and blowers). The additional power demand for the unit operations not available in the process simulation (ex. minor process pumping, odour control, process control equipment, etc.) were quantified by subtracting the power demand of the calibrated model from the total power demand calculated from the field data. The power demand intensities used for each process units' simulation are listed in Appendix C. The supplemental natural gas used for power generation was also accounted for here. The cogeneration system power and thermal energy efficiencies were also calibrated based on the field values that were either provided directly by the facility or calculated from the energy balance using the facility data.

The trickling filters were not modelled dynamically here due to them not varying in operating conditions between the scenarios to prevent them from inevitably burdening the simulation computational speed. However, their electricity demand was entered into the model to estimate their contribution to the facility's total power demand. The effluent characteristics of the trickling filters and activated sludge units were assumed to be the same. To optimize the simulation's run time, the entire facility was divided into 6 identical trains and only one of these trains was simulated. The results of the single-line simulations were subsequently scaled up to the total by multiplying times the number of actual units.

To perform the dynamic simulation, hourly influent profiles including at least flow, chemical oxygen demand (COD), and total Kjeldahl nitrogen (TKN) concentration are required. The facility data collection system recorded only monthly averages. As such, the simulation dynamic hourly input profiles were developed by multiplying these monthly averages by a calculated ratio (average instantaneous factors) developed from hourly flow data pattern provided by the facility (Fig. B.1). The typical CBOD/COD and Ammonium/TKN ratios (0.38 and 0.66 respectively) provided by the facility was used to reconstruct COD and TKN data trends from CBOD and ammonium measurements in absence of COD and TKN field data sets.

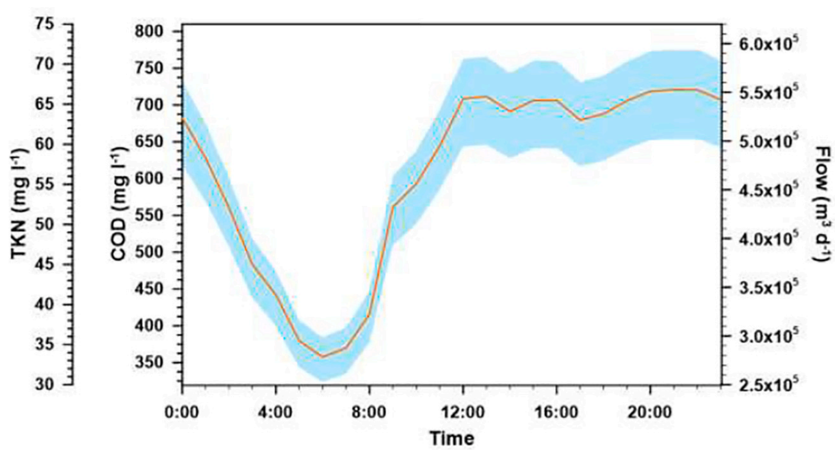

Fig. B.1. Current facility's influent dynamic trends for October 2018 through September 2019 derived from monthly averages and multiplied by average instantaneous hourly factors defined as the ratio of instantaneous to average flows [6]. All three Y-axis apply to the data points plotted. Shaded in blue is the range of the entities shown on each Y-axis during this 12-month period and the red line represents their hourly averages over one year.

In addition, average daily hourly ambient temperature data for October 2018 through September 2019 from the closest weather station to this facility [25] was compiled and used for these simulations. In absence of field data, the monthly temperature fluctuation of the wastewater was assumed to be a sinusoid with the minimum and maximum temperature of 20 °C and 30 °C occurring in March and September, respectively. The wastewater temperature was assumed to be constant during each month and influenced by ambient temperature with about 2 months delay based on previous research projects in this region.

The natural gas caloric value was derived from the default high heat value in the greenhouse gas (GHG) combustion emission calculation protocol by U.S. EPA, which is also used for GHG emission calculations in this study [17]. To determine the GHG emissions associated with the grid's electricity imports, the dynamic hourly average CO_2 intensity for the grid's electricity was calculated from data obtained from California Independent System Operator's (CAISO) for each month of the year [16]. These hourly trends for different months of 2019 were developed by Firouzian et al., 2022 and were utilized for the dynamic simulation performed in this article [6].

In addition to electricity importation (indirect GHG emissions), following direct GHG emissions were calculated and accounted for in this study: CO_2, N_2O, and CH_4 emissions associated with activated sludge biological treatment; CO_2 emission associated with sludge digestion; combustion of biogas and natural gas; and CH_4 from biogas fugitive leaks. Fugitive methane emission or biogas leak was assumed to be 1 % of the total methane generation in the digesters. The total GHG emission was reported as CO_2eq units, by multiplying each mass flow times the respective global warming potential from U.S. EPA [26].

The cost of power imported from the grid was calculated using SCE's tariffs presented in Appendix A (from Firouzian et al., 2022) and net power demand values calculated by the simulation for each hour of the study period. For this calculation, summer tariffs were applicable to June 1 through September 30 [20]. Same metering, energy usage (delivery and generation), and fixed and time related demand charges as what utilized by Firouzian et al., 2022 were used to calculate the cost of imported electricity for the two scenarios discussed here.

The costs of chemicals were calculated and accounted for using the software's defaults [18] except for the anionic polymers consumed at chemically enhanced primary treatment (CEPT) whose cost (32.13 USD per 1000 m^3 of primary treatment influent) was obtained from the vendor (NSF Polydyne Inc.; Riceboro, GA) per Firouzian et al., 2022. Among the different chemicals used at this facility, only the ferric chloride and anionic polymers used for the primary treatment enhancement and chemical additives used in sludge dewatering and thickening processes were accounted for here. Biosolid disposal cost was also accounted for and calculated using the default cost option for dry sludge disposal (cost per unit mass of TSS) in the simulation software [18].

Appendix C. Process parameters used for simulations

Tables below summarize the specifications and parameters used for simulation in addition to the simulation software's defaults:

Table C.1
Primary treatment specifications.

Process unit	Process parameter	Step-feed (NDN)	Plug-flow (C-ox)
Primary clarifier	Total Basins Count	26	26
	Basins Count in Service	20	20
	Volume per Basin (1000 m^3)	1.9	1.9
	Depth (m)	2.7	2.7
	Width (m)	12.0	12.0
	Length (m)	58.4	58.4
	Clarifier Model Parameters Used for CEPT:		
	BioWin CEPT Default Max Vesilind Settling Velocity (m/d)	150.0	150.0
	BioWin CEPT Default Vesilind Hindered Zone Settling Parameter (L/g)	0.40	0.40
	Calibrated Clarification Switching function (mg/L)	618.0	618.0
	BioWin CEPT Default Max Compactability Slope (mg/L)	50,000.0	50,000.0
	Clarifier Model Parameters Used for Conventional Clarifiers (non-CEPT)	N/A	N/A

Table C.2
Secondary treatment specifications – activated sludge configurations.

Process unit	Process parameter	Step-feed (NDN)	Plug-flow (C-ox)
Activated sludge	Total Basins Count	10	10
	Count of Basins in Service	10	10
	Volume per Basin (1000 m^3)	5.3	5.3
	Zone Volume Breakdown (1000 m^3):		
	Zone 1A	0.42	0.42
	Zone 1B	0.42	0.42
	Zone 2	0.82	0.82
	Zone 3	0.82	0.82
	Zone 4	0.92	0.92
	Zone 5	0.92	0.92
	Zone 6	0.92	0.92
	Depth (m)	4.57	4.57
	Width (m)	14	14
	Length (m)	83.8	83.8
	Fine Bubble Diffusers Diameter (m)	0.18	0.18
	Coarse Bubble Diffusers Diameter (m)	BioWin's Default [18]	BioWin's Default [18]
	Diffuser Count per Zone per Basin:		
	Zone 1A	Anoxic w/ 6 Coarse Bubble Diffusers	866
	Zone 1B	866	866
	Zone 2	1732	1732
	Zone 3	Anoxic	1732
	Zone 4	1732	1732
	Zone 5	1732	1000
	Zone 6	1626	1000
Activated sludge secondary clarifier	Total Basins Count	26	26
	Count of Basins in Service	26	26
	Volume per Basin (1000 m^3)	2.95	2.95
	Depth (m)	4.88	4.88
	Width (m)	13.2	13.2
	Length (m)	45.9	45.9
	Clarifier Model Parameters Used for non-CEPT	BioWin's Default [18]	BioWin's Default [18]

Table C.3
Digesters and sludge processing specifications.

Process unit	Process parameter	Step-feed (NDN)	Plug-flow (C-ox)
Digesters:			
Small Digester	Total Digester Count	2	2
	Count of Digesters in Service	1	1
	Volume per Digester (1000 m^3)	5.35	5.35
	Digester Head Space (% of Total Volume)	16 %	16 %
	Height (m)	9.14	9.14
	Digester Wall Thickness (% of Diameter)	15.1 %	15.1 %
	Diameter (m)	32.2	32.2
Large Digesters	Total Digester Count	8	8
	Count of Digesters in Service	8	8
	Volume per Digester (1000 m^3)	7.28	7.28
	Digester Head Space (% of Total Volume)	16 %	16 %
	Height (m)	9.14	9.14
	Digester Wall Thickness (% of Diameter)	15.1 %	15.1 %
	Diameter (m)	37.5	37.5
Digested Sludge Dewatering	% Removal	Dynamic trend derived from field monthly data post calibration.	Dynamic trend derived from field monthly data post calibration.
Digester Heat Loss per Year (C/day)	October 2018 through April 2019 (post Calibration)	0.145	0.145
	May 2018 through September 2019 accounting for additional natural gas import for electricity peak shaving (post Calibration)	0.957	0.957
Sludge Thickeners	Primary Sludge % Removal	99.78 %	99.78 %
	Secondary Sludge % Removal	99.78 %	99.78 %

Table C.4
Energy calculations specifications.

Process unit	Process parameter	Step-feed (NDN)	Plug-flow (C-ox)
Blower	Efficiency	59.00 %	59.00 %
Cogeneration	%Fuel Energy Converted to Power	35.00 %	35.00 %
	Cogeneration Heat Recovery Steam Generator Heat Transfer Efficiency	55.0 %	55.0 %
	%Fuel Energy Converted to Heat in Cogeneration (not accounting for heat exchanger efficiency)	18.18 %	18.18 %
	Natural Gas Boiler Efficiency	60.0 %	60.0 %
	Natural Gas LHV (kJ/kg)	51,810	51,810
	Pure Methane LHV (kJ/kg)	50,000	50,000
	Natural Gas HHV/LHV Ratio	1.1100	1.11

Table C.5
Power demand intensities (power demand per unit flow of wastewater treated) for each process unit replaced the defaults in the simulation software.

Process unit	Power intensity (Wh/m^3)	Source of factor
Primary Clarifier	2.09E+01	Derived from Plant Data
Influent Lift Pumps	7.84E+01	Derived from Plant Data
Other Power Consumption (ex, pumping, odour control, control system, etc.)	5.27E+01	Derived from Plant Data
Secondary Clarifier	1.60E+01	[27]
Trickling Filters	1.47E+02	[28]
Digester (Mixing and Biogas Compression)	6.30E+02	Derived from Plant Data
Thickening (Centrifuge)	6.19E+02	[27]
Digested Sludge Dewatering (Centrifuge)	4.15E+03	[27]
Rotating Belt Filter Driver Train and Pumping	8.60E+01	[27]
Primary Filter Driver Train and Pumping	8.78E+01	[27]

Appendix D. Effluent dynamic trends

Simulations for both plug-flow (C-ox) and step-feed (NDN) scenarios were completed using dynamic influent profiles, process specifications, and time-dependent alpha diurnal schedule for each aerated reactor as discussed in the Materials and methods section. The effluent concentration trends for TSS, CBOD, ammonium, nitrate, and total nitrogen for these two scenarios have been compared in Figs. D.1 through D.5 below:

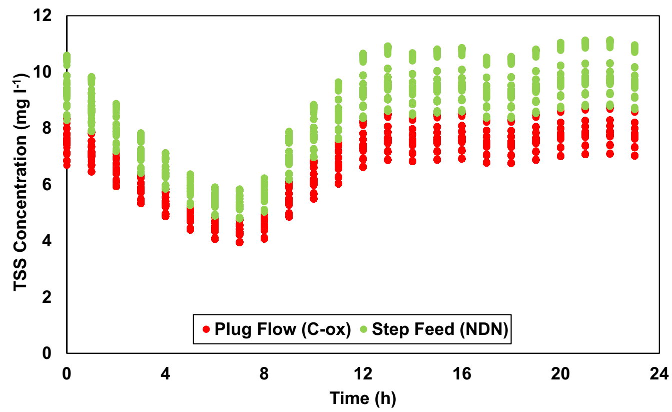

Fig. D.1. Facility's effluent TSS concentration comparison for these two scenarios.

The higher step-feed configuration's TSS in Fig. D.1 above can be explained by its higher mean cell residence time (MCRT) which is required for the growth and performance of nitrogen removing microorganisms (i.e., Autotrophs). The historical field data used for modelling of these two legacy configurations included average MCRT of 4.7 and 1.1 days for the step-feed and plug-flow configurations, respectively. The higher MCRT in the step-feed configuration is achieved by increase of the flow in the activated sludge recycle stream (RAS) that is sent back to the beginning of the activated sludge basin as a result of the reduction in the waste activated sludge (WAS) stream which is sent to digesters. This higher recycling of activated sludge in the step-feed scenario increases the concentration of solids in the activated sludge reactors (a.k.e., mixed liquor suspended solids or MLSS); thus, increases the load of the solids that enter the secondary clarifiers which translates into higher effluent TSS concentration.

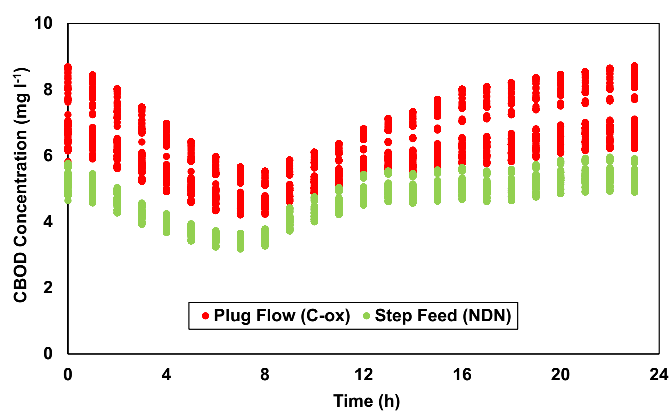

Fig. D.2. Facility's effluent CBOD concentration comparison for these two scenarios.

The higher CBOD concentration in the effluent of plug-flow scenario in Fig. D.2 above can be also explained by the higher MCRT of step-feed which increases the number of carbon consuming microorganism in the system (i.e., Heterotrophs and Autotrophs) resulting in higher extent of CBOD removal in the step-feed configuration.

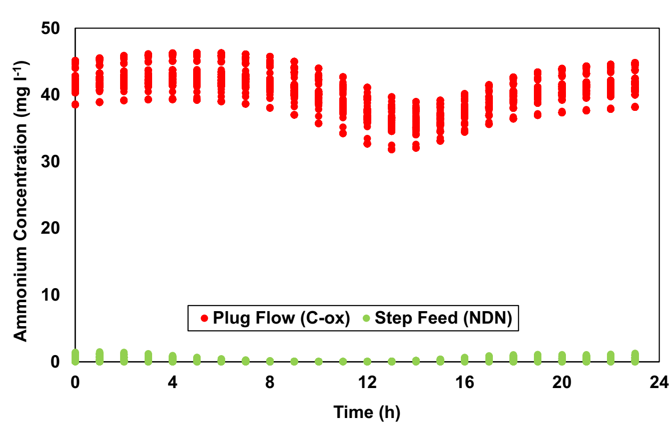

Fig. D.3. Facility's effluent N-NH_4^+ concentration comparison for these two scenarios.

Since nitrification and denitrification (i.e., nitrogen oxidation and removal) cannot be performed at low MCRT of the plug-flow configuration, higher concentration of ammonium ($NH4^+$) is observed in the effluent of this configuration in Fig. D.3 comparing to negligible traces in the step-feed's. Same explanation can be provided for zero concentration of nitrate (NO_3^-) observed in the effluent of plug-flow configuration in the Fig. D.4 below.

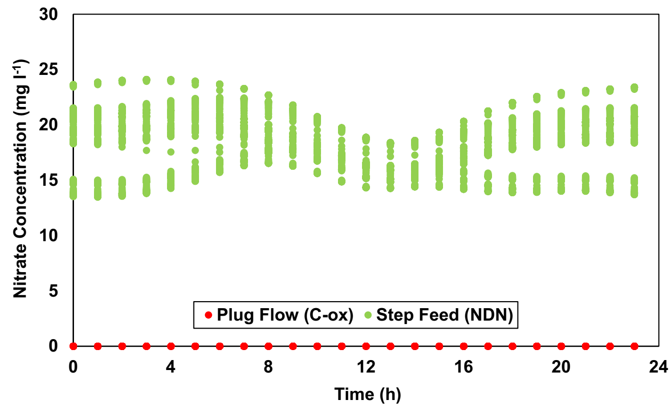

Fig. D.4. Facility's effluent N-NO_3^- concentration comparison for these two scenarios.

Fig. D.5 below illustrates the total nitrogen concentrations of these options. It also allows cumulative comparison of extent of nitrogen removal for these two scenarios that treat almost the same amount of influent nitrogen (Fig. B.1 and close influent flows of these scenarios). As explained in the comparison of N-NH_4^+ and N-NO_3^- above, plug-flow's MCRT does not allow nitrification and denitrification thus its nitrogen removal is limited to nitrogen content of the sludge removed through this scenario's primary and secondary settling. As such, the average 50 % lower total nitrogen concentrations of step-feed could be explained to be the result of nitrification and denitrification in this scenario whose secondary sludge removal is even less than plug-flow's (i.e., less nitrogen removal through solids removal).

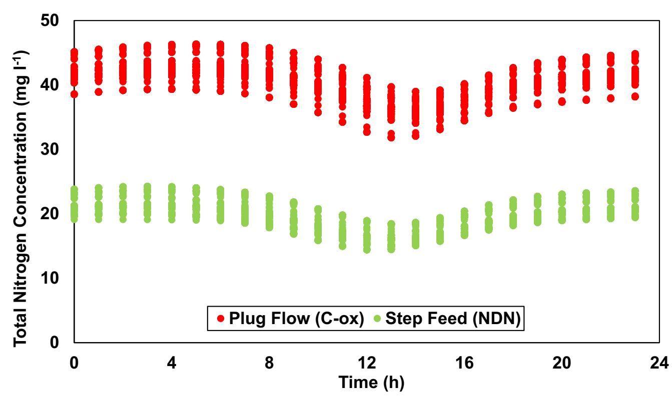

Fig. D.5. Facility's effluent N-Total Nitrogen concentration comparison for these two scenarios.

Appendix E. Effluent quality index

Effluent quality index (EQI) defined as weighted sum of the pollutants in the effluent [21,22] is calculated as following:

$$EQI = 1 \Big/ (\Delta t.1000) \int_{t_1}^{t_2} \left[\beta_{TSS}.TSS_e(t) + \beta_{COD}.COD_e(t) + \beta_{TKN}.TKN_e(t) + \beta_{NO_3^-}.NO_{3e}^-(t) + \beta_{BOD_5}.BOD_{5e}(t)\right] Q_e(t)dt \tag{E.1}$$

where Δt is the total evaluation period; $Q_e(t)$ is instantaneous effluent flow rate during the evaluation period; $TSS_e(t)$, $COD_e(t)$, $TKN_e(t)$, $NO_{3e}^-(t)$, $BOD_{5e}(t)$ are these wastewater constituents' instantaneous concentrations in the effluent; β represents weighted factors for different wastewater constituent which are $\beta_{TSS} = 2$, $\beta_{COD} = 1$, $\beta_{TKN} = 30$, $\beta_{NO_{3e}^-} = 10$, $\beta_{BOD5} = 2$ [21,22]. 1000 is the unit conversion factor which can be replaced by other factors depending on the desired unit for EQI.

Using the same logic as EQI's, influent quality index (IQI) can be defined as following:

$$IQI = 1 \Big/ (\Delta t.1000) \int_{t_1}^{t_2} \left[\beta_{TSS}.TSS_i(t) + \beta_{COD}.COD_i(t) + \beta_{TKN}.TKN_i(t) + \beta_{NO_3^-}.NO_{3i}^-(t) + \beta_{BOD_5}.BOD_{5i}(t)\right] Q_i(t)dt \tag{E.2}$$

where Δt is the total evaluation period; $Q_i(t)$ is instantaneous influent flow rate during the evaluation period; $TSS_i(t)$, $COD_i(t)$, $TKN_i(t)$, $NO_{3i}^-(t)$, $BOD_{5i}(t)$ are these wastewater constituents' instantaneous concentrations in the influent; β represents weighted factors for different wastewater constituent which are $\beta_{TSS} = 2$, $\beta_{COD} = 1$, $\beta_{TKN} = 30$, $\beta_{NO^-_{3e}} = 10$, $\beta_{BOD5} = 2$ [21,22]. 1000 is the unit conversion factor which can be replaced by other factors depending on the desired unit for IQI.

Using the equations above quality index removal (QIR) is defined as:

$$QIR = IQI - EQI \tag{E.3}$$

References

[1] D.J. Reardon, Turning down the power, Civ. Eng. 65 (8) (1995) 54–56.
[2] G. Olsson, Water and Energy: Threats and Opportunities, 2nd ed., IWA Publishing, London, UK, 2015.
[3] H.O.R. Howlader, M. Furukakoi, H. Matayoshi, T. Senjyu, Duck curve problem solving strategies with thermal unit commitment by introducing pumped storage hydroelectricity & renewable energy, in: 2017 IEEE 12th International Conference on Power Electronics and Drive Systems (PEDS), Honolulu, HI, 2017, p. 2017.
[4] H.O.R. Howlader, M.M. Sediqi, A.M. Ibrahimi, T. Senjyu, Optimal thermal unit commitment for solving duck curve problem by introducing CSP, PSH and demand response, IEEE Access 6 (2018) 4834–4844.
[5] M.A. Gonzalez-Salazar, T. Kirsten, L. Prchlik, Review of the operational flexibility and emissions of gas- and coal-fired power plants in a future with growing renewables, Renew. Sustain. Energy 82 (2018) 1497–1513.
[6] M. Firouzian, M. Stenstrom, D. Rosso, Effects of power tariffs and aeration dynamics on the expansion of water resource recovery facilities, Clean. Prod. (2022) 1–13.
[7] A. Zohrabian, S. Plata, D. Kim, A.E. Childress, K.T. Sanders, Leveraging the water-energy nexus to derive benefits for the electric grid through demand-side management in the water supply and wastewater sectors, Wiley Interdiscip. Rev. Water 8 (3) (May 2021) 1–23.
[8] E. Musabandesu, F. Loge, Load shifting at wastewater treatment plants: a case study for participating as an energy demand resource, J. Clean. Prod. 282 (2021).
[9] D. Rosso, M. Stenstrom, Comparative economic analysis of the impacts of mean cell retention time and denitrification on aeration systems, Water Res. 39 (16) (2005) 3773–3780.
[10] D. Rosso, M. Stenstrom, Energy-saving benefits of denitrification, Environ. Eng. 43 (3) (2007) 29–38.
[11] L. Rieger, S. Gillot, G. Langergraber, T. Ohtsuki, A. Shaw, I. Takacs, S. Winkler, Guidelines for Using Activated Sludge Models, IWA, London, 2013.
[12] American Society of Civil Engineers, ASCE Standard ASCE/EWRI 18-18, in: Standard Guidelines for In-Process Oxygen Transfer Testing, American Society of Civil Engineers, Reston, VA, 2018.
[13] D. Rosso, D.L. Huo, M.K. Stenstrom, Effects of interfacial surfactant contamination on bubble gas transfer, Chem. Eng. Sci. 61 (16) (2006) 5500–5514.
[14] D. Bencsik, I. Tak'acs, D. Rosso, Dynamic alpha factors: prediction in time and evolution along reactors, Water Res. 216 (118339) (June 2022).
[15] L.M. Jiang, M. Garrido-Baserba, D. Nolasco, A. Al-Omari, H. DeClippeleir, S. Murthy, D. Rosso, Modelling oxygen transfer using dynamic alpha factors, Water Res. 124 (2017) 139–148.
[16] California Independent System Operator, Today's outlook [Online]. Available: http://www.caiso.com/TodaysOutlook/Pages/index.html, 22 05 2021.
[17] U.S. EPA, Title 40 part 98—mandatory greenhouse gas reporting-subpart C—general stationary fuel combustion sources [Online]. Available: https://www.ecfr.gov/cgi-bin/text-idx?SID=c928f22246db4fd098e7ed7cdf75a869&mc=true&node=pt40.23.98&rgn=div5#sp40.23.98.c, 12 09 2016.
[18] EnviroSim, BioWin 6.1 Help Manual, EnviroSim, Hamilton, Ontario, 2020.
[19] U.S. EPA, Region 4 Laboratory Services and Applied Sciences Division, Wastewater Flow Measurement Operating Procedure, Athens, Georgia, 2020.
[20] Southern California Edison, SCE-document library [Online]. Available: https://library.sce.com/?10000_group.propertyvalues.property=jcr%3Acontent%2Fmetadata%2Fcq%3Atags&10000_group.propertyvalues.operation=equals&10000_group.propertyvalues.0_values=sce-document-library%3Aregulatory%2Fsce-tariff-books%2Felectric%2Fschedules%2, 22 05 2021.
[21] U. Jeppsson, M.-N. Pons, I. Nopens, J. Alex, J. Copp, K. Gernaey, C. Rosen, J.-P. Steyer, P. Vanrolleghem, Benchmark simulation model no 2: general protocol and exploratory case studies, Water Sci. Technol. 56 (8) (2007) 67–78.
[22] I. Nopens, L. Benedetti, U. Jeppsson, M.-N. Pons, J. Alex, J.B. Copp, K.V. Gernaey, C. Rosen, J.-P. Steyer, P.A. Vanrolleghem, Benchmark Simulation Model No 2: finalisation of plant layout and default control strategy, Water Sci. Technol. 62 (9) (2010) 1967–1974.
[23] L. Tseng, A.K. Robinson, X. Zhang, X. Xu, J. Southon, A.J. Hamilton, R. Sobhani, M. K. Stenstrom, D. Rosso, Identification of preferential paths of fossil carbon within water resource recovery facilities via radiocarbon analysis, Environ. Sci. Technol. 50 (2016) 12166–12178.
[24] G.A. Baquero-Rodríguez, S. Martínez, J. Acuña, D. Nolasco, D. Rosso, How elevation dictates technology selection in biological wastewater treatment, J. Environ. Manag. 307 (2022) 114588.
[25] Weather Underground, John Wayne Airport Station [Online]. Available: https://www.wunderground.com/history/monthly/us/ca/santa-ana/KSNA/date/2018-10, 22 05 2021.
[26] U.S. EPA, Title 40 part 98—mandatory greenhouse gas reporting-subpart A—general provision [Online]. Available: https://www.ecfr.gov/cgi-bin/text-idx?SID=c928f22246db4fd098e7ed7cdf75a869&mc=true&node=pt40.23.98&rgn=div5#sp40.23.98.a, 11 12 2014.
[27] S. Pabi, A. Amarnath, R. Goldstein, L. Reekie, Electricity Use and Management in the Municipal Water Supply and Wastewater Industries, Electric Power Research Institute & Water Research Foundation, Palo Alto, California, 2013.
[28] R. Sobhani, L.-M. Jiang, A.M. Chau, J. Brown, E. Torres, Y. Shao, D. Rosso, Energy Footprint Analysis of Orange County Sanitation District's Operations, Water Environment Federation, Los Angeles, 2011.